

## Removal of Antibiotic Sulfamethazine from Aqueous Media Using Watermelon Seeds as a New Low Cost and Ecofriendly Adsorbent

I. Nadir, Y. Achour\*, A. El Kassimi, M. El Himri, M.R. Laamari and M. El Haddad\*

*Laboratoire de Chimie Analytique et Moléculaire, Faculté Poly-disciplinaire, Université Cadi Ayyad, BP 4162, 46000 Safi, Maroc*

*(Received 25 September 2020, Accepted 7 December 2020)*

The removal efficiency of sulfamethazine, as a representative antibiotic (SMT), on a new and eco-friendly activated carbon provided from watermelon seeds as adsorbent has been studied in simple systems. Some experimental parameters, namely pH, the amount of adsorbent and contact time are studied. Based on the results, the weak chemical bonds ( $\pi$ - $\pi$  EDA interactions) are responsible for the adsorption of SMT to watermelon seeds. The present adsorbent played an important role in the sorption of SMT, leading to a higher sorption capacity onto the watermelon seeds ( $90.78 \text{ mg g}^{-1}$ ). The solvent effect is been studied to show that the electron-donor-acceptor (EDA) interaction is the main adsorption mechanism of SMT antibiotic and that adsorption capacity increases with the increase of dipole moment of solvents. A kinetic study showed that the removal efficiency process followed the pseudo-second-order model and the Langmuir isotherm was the best model to fit and describe the phenomenon in the single system.

**Keywords:** Adsorption, Antibiotic SMT, Isotherms, Kinetics, Mechanism study, Thermodynamic studies, Watermelon seeds

### INTRODUCTION

Water pollution by certain industrial chemicals is a source of environmental degradation [1]. Currently, pollution is of particular interest at the international level. The remediation of water contaminated by antibiotics is necessary for the protection of environment [2,3].

Water contamination by antibiotics is becoming a worldwide environmental issue. Antibiotic compounds, belonging to emerging pollutants, are consumed for therapeutic prevention [4]. These contaminants cause toxicity mainly to aquatic fauna and flora even at low concentrations, such as micrograms per liter to nanograms per liter. Although sewage disposal is known as the main source of toxic materials, eco-toxicological effects caused by pharmaceutical compounds present in wastewater and sewage are not completely understood [5,6].

Particularly, sulfonamides (SNs) have been widely used

in human and veterinary medicine to treat and prevent infectious bacterial diseases. These sulfonamides are often discharged into aquatic environments *via* domestic wastewater effluents, disposal of expired pharmaceuticals, and excretion in its original or metabolized form [17].

Sulfamethazine (SMT), a commonly used SN antibiotic, was chosen as the target contaminant due to its large global consumption in the animal food industry. SMT is classified as an emerging substance by the network of reference laboratories, research centers and related organizations for monitoring the emerging environmental substances not included in the European water-monitoring program that could be a promising candidate for future regulation. The systematic name of SMT is 4-amino-N-[4,6-dimethyl-2-pyrimidinyl] benzenesulfonamide). It is commonly used in veterinary medicines in high concentrations. As a major SN drug, SMT is extensively used to control infectious diseases as well as treatment. SMT and its by-products have been identified along with other pharmaceuticals in the secondary wastewater effluents. Although they have little or no direct effects on human health, the risk of developing antibiotic-

\*Corresponding authors. E-mail: [youness.achour@gmail.com](mailto:youness.achour@gmail.com); [elhaddad71@gmail.com](mailto:elhaddad71@gmail.com)

resistant bacteria has been reported. Therefore, it is important to develop efficient treatment technologies to control the concentration level of SMT in aquatic environments. SMT is an important antibiotic used in swine treatment applied for urinary, ear and skin infections. It is excreted 24 h after ingestion, and about 35% is excreted non-metabolized, thus presenting health risk for aquatic animals, humans and the environment. However, there is no legislation to regulate SMT sewage discharge in sewage and wastewaters.

To this end, many treatment techniques have been developed. Among these methods are electrocoagulation [9], membrane filtration, advanced oxidation process, electrochemical destruction, ozonation, precipitation, exchange of ions, biological methods, coagulation/flocculation [10], *etc.*; however, these technologies are expensive. It should be noted that adsorption is a simple, low cost and effective method to treat industrial wastewater.

Advantages of adsorption technique, including low cost, no by-product formation and easy operational process, make it an effective way to remove antibiotics in wastewater [12] [13]. In the aqueous system, the complexity of the SMT speciation indicates the complexity of the sorption behavior during its removal. Moreover, the results of many experiments performed show that sulfonamides are not easy to be adsorbed and not easy to be biodegraded; they are leachable materials. The neutral form of SMT predominates between pH 3 and 7. SMT exists in water *via* several forms including uncharged molecule (SMT<sub>0</sub>), zwitterion (SMT<sup>±</sup>), cation (SMT<sup>+</sup>) and anion (SMT<sup>-</sup>), owing to proton exchange of aromatic amine and sulfonamide groups on molecule [11]. Varieties of mechanisms of SMT sorption including hydrophobic partitioning, cation exchange and complex surface reactions (hydrogen bonding and other polar interactions) between the functional groups (carboxyl, phenol, and amino) of the adsorbate molecules have been proposed [8]. Sorption behaviors of SMT have been investigated on materials such as graphene oxide-coated biochar nanocomposites [14], green microalga [15], magnetic Fe<sub>3</sub>O<sub>4</sub>/red mud-nanoparticles [16], steam-activated invasive plant-derived biochar [17], hexadecyl trimethyl ammonium bromide modified activated carbon [18] and

magnetic yolk-shell mesoporous carbon architecture [19].

The most common problems encountered during the adsorption process of SMT are generally related to the adsorption capacity of SMT, due to the specific surface of the used adsorbent; also, the adsorption kinetics can be an essential parameter in some processes. Therefore, the resistance to pH solution and temperature can be essential factors in the adsorbent resistance. Finally, the dominate mechanisms for adsorption of SMT must be taken into account during the study.

In this work, SMT was chosen as a model compound to investigate the adsorption behavior of sulfonamides in the activated watermelon seeds for wastewater treatment. The kinetics of SMT adsorption on activated watermelon seeds was determined through batch experiments. The effects of contact time, the concentration of SMT, pH and temperature on SMT adsorption were all examined in detail.

## MATERIALS AND METHODS

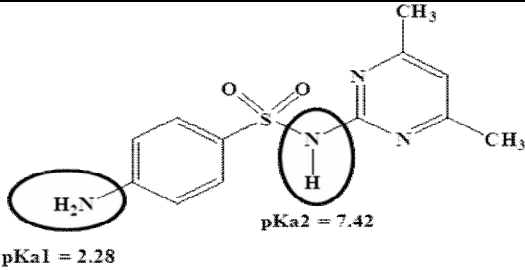
### Chemicals

SMT antibiotic was purchased from Sigma-Aldrich (St. Louis, MO, USA), and its physicochemical properties are presented in Table 1. A stock solution of 100 mg l<sup>-1</sup> was prepared from chemicals, specifically SMT (≥ 99 %). Working solutions were diluted from the stock solutions with double-distilled water.

### Preparation of Watermelon Seeds Adsorbent (WmS-500)

Watermelon seeds (WmS) were collected, washed several times with distilled water and dried at room temperature. The resulting material was activated with a mixture of phosphoric acid and double-distilled water with a mass ratio (1:4) in a glass beaker of 100 ml and heated oven at a temperature of 500 °C for two h to produce black carbonaceous residue, and the obtained material was neutralized at natural pH by distilled water. Then, the material was filtered, washed several times with distilled water, dried at 100 °C for two hours and kept in a desiccator for further use. The prepared adsorbent was abbreviated as WmS-500. The pH Zero Point Charge of WmS-500 is pH<sub>ZPC</sub> = 5.8 as described in reference [20].

**Table 1.** Physicochemical Properties of SMT

Properties	Sulfamethazine (SMT)
Chemical structure	 <p style="text-align: center;">pKa1 = 2.28      pKa2 = 7.42</p>
Molecular formula	C <sub>12</sub> H <sub>14</sub> N <sub>4</sub> O <sub>2</sub> S
CAS reg. no	57-68-1
Molecular mass	278.33 g mol <sup>-1</sup>
Water solubility	1.5 mg ml <sup>-1</sup>
pK <sub>a</sub>	2.28 and 7.42
Wavelength	275 nm
Therapeutic class	Sulfonamide
Mode of action	Inhibiting the bacterial synthesis of dihydrofolic acid by competing with <i>para</i> -aminobenzoic acid for binding to dihydropteroate synthase (dihydrofolate synthase). Inhibition of dihydrofolic acid synthesis decreases the synthesis of bacterial nucleotides and DNA

### Adsorption Experiments

The adsorption study of SMT onto WmS-500 adsorbent was achieved by batch experimental technique on a thermostated shaker. Percentage of the removal and adsorbed amount of SMT antibiotic were calculated using Eqs. (1) and (2), respectively:

$$\%SMT\ Removal = \frac{C_0 - C_e}{C_0} \cdot 100 \quad (1)$$

$$q_e = \frac{C_0 - C_e}{m} \cdot V \quad (2)$$

where  $q_e$  is the adsorbed amount of antibiotic at equilibrium (mg/g),  $C_0$  is the initial concentration of SMT (mg l<sup>-1</sup>),  $C_e$  is the equilibrium concentration of SMT (mg l<sup>-1</sup>),  $m$  is the amount of WmS-500 adsorbent (g) and  $V$  is the solution

volume (l).

The adsorption experiments of SMT onto WmS-500 adsorbent were conducted as follows: 50 ml of the SMT antibiotic solution 1000 mg l<sup>-1</sup> was prepared into 250 ml flasks to investigate the pH influence on the adsorption. The pH of the solutions was adjusted from 2 to 14 using 0.1 M (HCl) and 0.1 M (NaOH) solutions, then 25 mg of WmS-500 adsorbent was added. The mixture was shaken at 130 rpm for 24 h. The effluent was filtered through a 0.2 μm filter paper. The effects of adsorbent dosage (5, 10, 15, 20, 25 and 30 mg) on adsorption efficiency of SMT onto WmS-500 adsorbent were also examined. Different amounts of adsorbent were added to a 50 ml solution of the SMT antibiotic solution at 25 mg l<sup>-1</sup>.

### Characterization

The chemical analysis of WmS-500 was performed

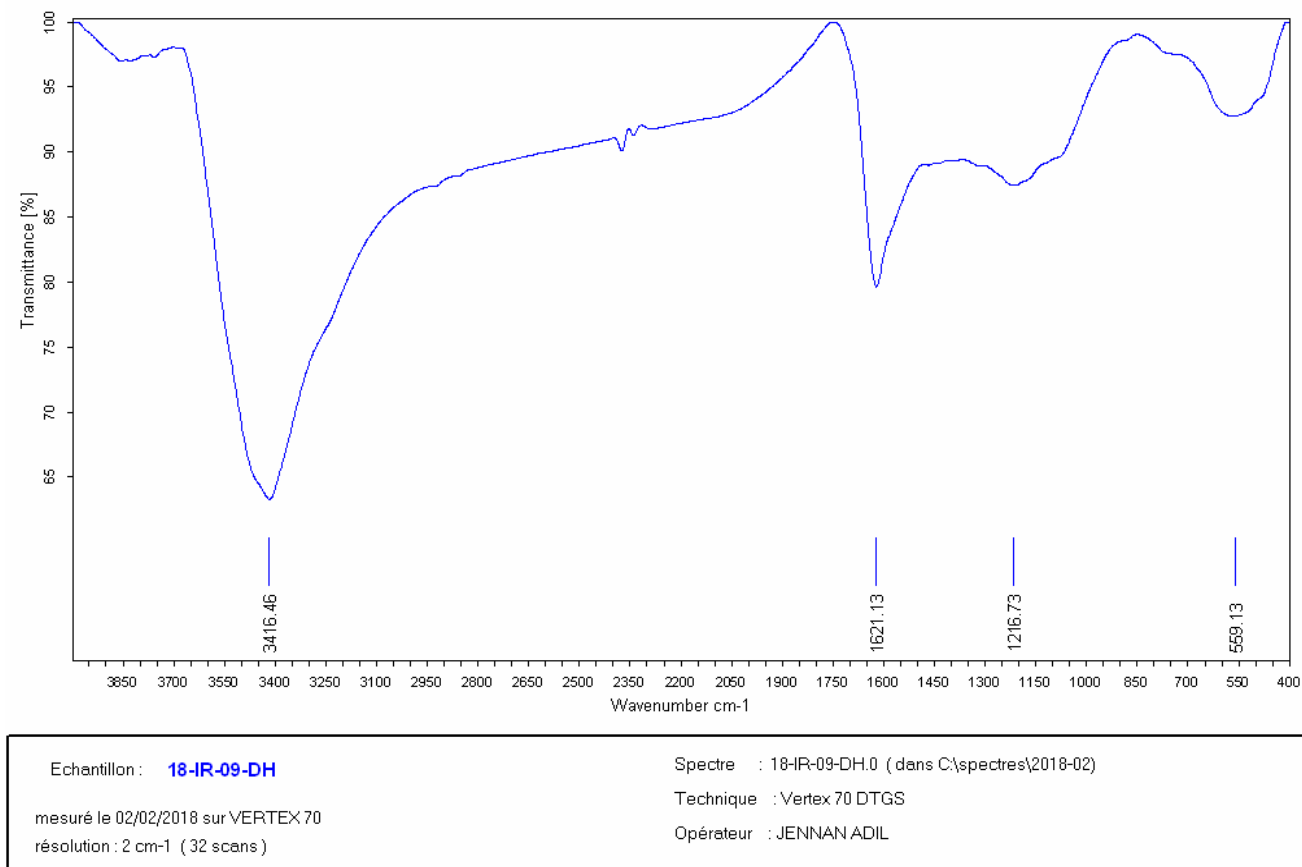


**Fig. 1.** Infrared spectrum of WmS-500 adsorbent.

using a Fourier transform infrared (FTIR) spectrum of the sample that was recorded on an FTIR spectrometer (Nicolet 5700 FT-IR spectrometer, Thermo Corp USA) using a standard KBr pellet technique. The morphology of the WmS-500 adsorbent was studied using the scanning electron microscope (SEM) technique, obtained with equipment (HITACHI-S4100, JAPAN). The images of the microstructure were obtained with a maximum voltage of 20 kV. The elemental composition was determined by energy dispersive spectroscopy (EDAX); determination of grain compositions with 10  $\mu\text{m}$  resolution.

## RESULTS AND DISCUSSION

### Characterization of Adsorbent

Figure 1 depicts the infrared spectrum of WmS-500

adsorbent. The frequencies of the absorption bands 559, 1216, 1621 and 3418  $\text{cm}^{-1}$  were selected for this spectrum. The absorption band at 3418  $\text{cm}^{-1}$  is attributed to the vibrations of the hydroxyl groups OH and NH stretching vibrations, the band at 2374  $\text{cm}^{-1}$  is attributed to the group C=O stretching vibrations of carboxylic acids, and the band at 1623  $\text{cm}^{-1}$  are attributed to the group C=C aromatic skeletal stretching, The band at 1076  $\text{cm}^{-1}$  is due to the group P=O, and a band at 558  $\text{cm}^{-1}$  is attributed to the C-C stretching vibrations. The absorption band at 3416  $\text{cm}^{-1}$  is attributed to the vibrations of the OH hydroxyl groups and NH stretching vibrations [21]. The band at 1621  $\text{cm}^{-1}$  is attributed to the C=C aromatic skeletal stretching, and the band at 1216  $\text{cm}^{-1}$  is ascribed to C-O stretching in alcohol, ether, hydroxyl group [22] [23]. Finally, the band at 559  $\text{cm}^{-1}$  is attributed to the C-C stretching vibrations [24].

Microscopic observation makes it possible to visualize the morphology of the ground material. Figure 2 shows that the ground material consists of agglomerates of small particles and grains. Therefore, it indicates that the surface contains many pores with different sizes and shapes.

The elemental composition of the material is illustrated by the spectrum in Fig. 3. It shows the presence of carbon, oxygen, potassium, silica and calcium in different amounts. The mass and atomic percentages of these elements are summarized in Table 2.

### Effect of WmS-500 Dosage on SMT Adsorption

The dependence of the adsorption of the antibiotic on the amount of WmS-500 adsorbent was studied at room temperature for each SMT removal by varying the adsorbent amount from 5 to 30 mg in contact with 50 ml solution of 10 mg l<sup>-1</sup> of SMT antibiotic. As shown in Fig. 4, the percentage removal of SMT increased by increasing the amount of WmS-500 adsorbent due to the greater availability of active sites in the layer of WmS-500 adsorbent. The adsorption efficiency increases with increasing time, and the response becomes constant for all the amounts used. The adsorption reached a maximum with 25 mg of the adsorbent amount, the maximum percentage removal was about 94%.

### Effect of pH

In Fig. 5, effects of solution pH on the SMT removal efficiency are summarized along with the speciation of SMT [25,26]. Removal percentages of SMT are plotted against solution pH. It can be seen from Fig. 5 that the dependencies of SMT removal on solution pH are related to the speciation of SMT. By considering the speciation of SMT or dissociation constants of SMT and pH at zero point charge for the WmS-500 adsorbent layer, the mechanism of SMT removal by adsorbent is examined as described below. SMT, consisting of one basic amine group (-NH<sub>2</sub>) and one acidic amide group (-NH-), has two dissociation constants that correspond to protonation of aniline N and deprotonation on SN NH, pK<sub>a1</sub> = 2.28 and pK<sub>a2</sub> = 7.42.

As seen in Fig. 5, the removal of SMT by WmS-500 adsorbent is dependent to the solution pH and is linked with the speciation of SMT. This behavior can be evaluated by considering relative contributions of speciation of SMT

changing with solution pH. The three forms of SMT can be expressed as follows:

$$\%SMT^0 = \frac{10^{-(pH+pK_{a1})}}{10^{-2pH} + 10^{-(pH+pK_{a1})} + 10^{-(pK_{a1}+pK_{a2})}} \cdot 100$$

$$\%SMT^+ = \frac{10^{-2pH}}{10^{-2pH} + 10^{-(pH+pK_{a1})} + 10^{-(pK_{a1}+pK_{a2})}} \cdot 100$$

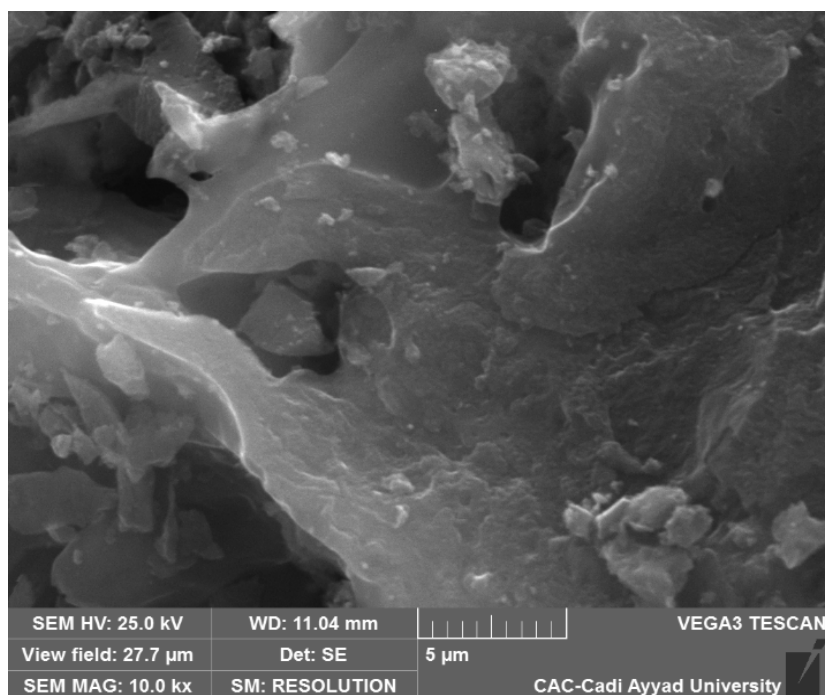
$$\%SMT^- = \frac{10^{-(pK_{a1}+pK_{a2})}}{10^{-2pH} + 10^{-(pH+pK_{a1})} + 10^{-(pK_{a1}+pK_{a2})}} \cdot 100$$

The chemical stability and altering the surface load of the adsorbent as well as the speciation of SMT in solution are the main reasons for strong dependence of SMT to pH. The material removal efficiency is also affected by the change in the pH of the solution due to the ionization state of the functional groups on the surface of the WmS-500 adsorbent. SMT having a speciation nature possesses two acid dissociation constants (pK<sub>a</sub>). The pK<sub>a1</sub> is ascribed to the ammonium group (-NH<sub>3</sub><sup>+</sup>), which can be observed in the pH range of 2-3, and pK<sub>a2</sub> can be attributed to the dissociation of (-SO<sub>2</sub>NH), a proton from the SMT group takes place at pH 7 to 11. As depicted in Fig. 5, the adsorption of SMT was enhanced with the pH increase from 2 to 7 and then abruptly decreased with the increase of pH. The reduced adsorption efficiency at high pH can be put forth to the shifting from cationic to anionic species. More possible adsorption mechanisms can occur as described in Fig. 6.

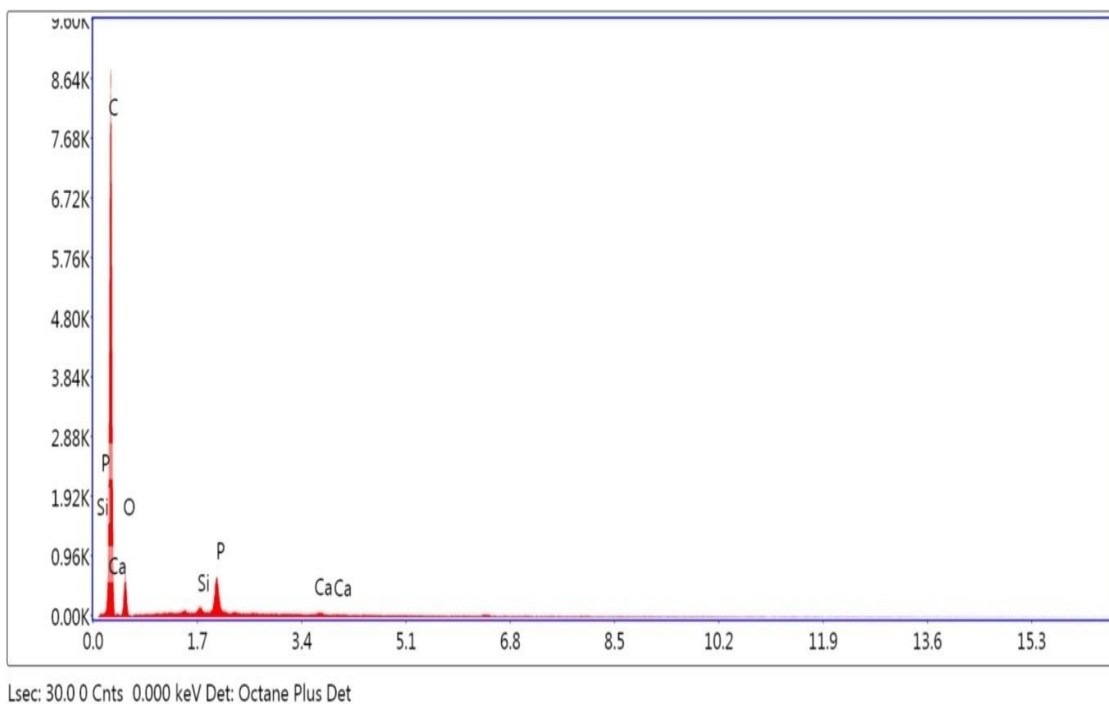
### Adsorption Mechanism

To better characterize and quantify the retention, it is necessary to focus on the phenomena occurring at the molecular scale; the adsorption mechanisms. Several possible interactions between WmS-500 adsorbent and SMT are responsible for the adsorption of antibiotics. Antibiotic/adsorbent linkages are hydrogen bonds, electrostatic interactions and electron donor-acceptor (EDA) interactions.

The hydrogen bond or hydrogen bridge is an intermolecular force involving a hydrogen atom and an electronegative atom such as oxygen, nitrogen and fluorine. Hydrogen bonds exist between carbon nonmaterial and adsorbate molecules when they have certain functional



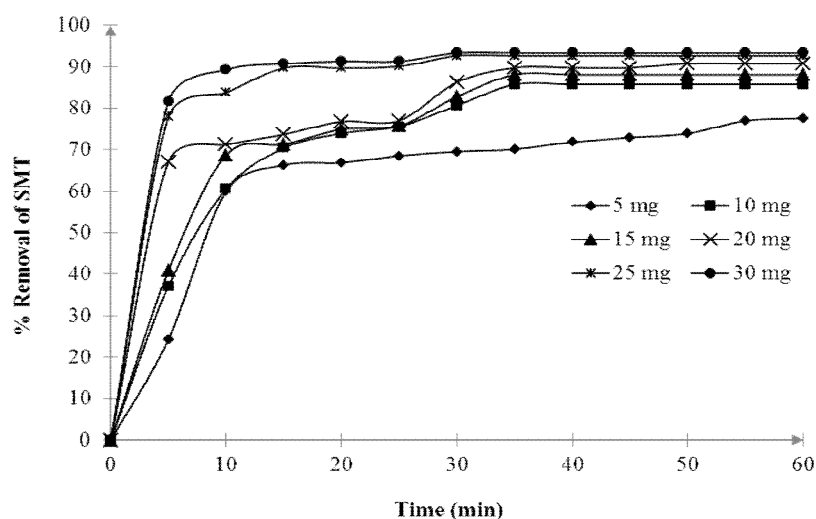
**Fig. 2.** SEM image of WmS-500 adsorbent.



**Fig. 3.** Spectrum of analysis by EDAX of WmS-500 adsorbent.

**Table 2.** Mass and Atomic Percentages of WmS-500 Adsorbent

Element	Weight (%)	Atomic (%)
C	80.4	85.1
O	17.7	14.1
Si	0.2	0.1
P	1.5	0.6
Ca	0.2	0.1

**Fig. 4.** Effect of adsorbent dosage on the removal efficiency of SMT onto WmS-500.

groups such as COOH, OH and NH<sub>2</sub> [27]. The infrared FTIR spectra of WmS-500 adsorbent before the adsorption of Fig. 1 show the existence of OH groups. SMT has an NH<sub>2</sub> group.

Therefore, according to the infrared spectra of WmS-500 adsorbent before and after SMT adsorption shown in Fig. 1, the peak at 3416 cm<sup>-1</sup> has disappeared or its intensity decreases. This peak is characterized by OH, so there is a hydrogen bridge with an electronegative element of SMT (nitrogen). However, hydrogen bonding was probably not the main cause of high adsorption capacity.

The molecular electrostatic attraction has also been used to interpret the adsorption of antibiotics on WmS-500

-adsorbent [28]. The effect of pH on the adsorption of antibiotics on WmS-500 adsorbent is shown in Fig. 6. It has been found that there must be other interactions stronger than the electrostatic interaction. Therefore, the electrostatic interaction is not the main interaction in the adsorption process

Based on the above analysis and the mechanism of antibiotics' adsorption, electron-acceptor donor (EDA) interaction has been proposed as the main mechanism of adsorption of antibiotics on WmS-500 adsorbent composites [28,29]. One type of EDA interaction is the interaction of  $\pi$ - $\pi$  EDA. The EDA interaction is specific and non-covalent, that exists between electron-rich compounds and electron-

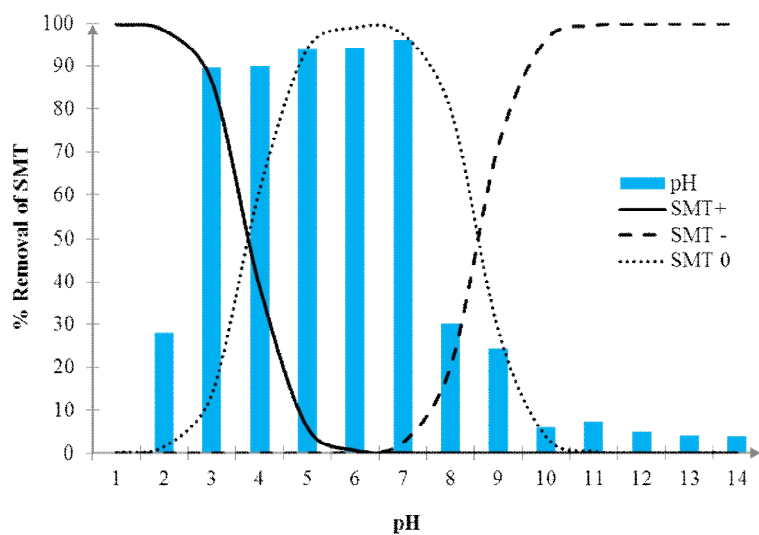


Fig. 5. Effect of pH on the SMT removal onto the WmS-500 adsorbent.

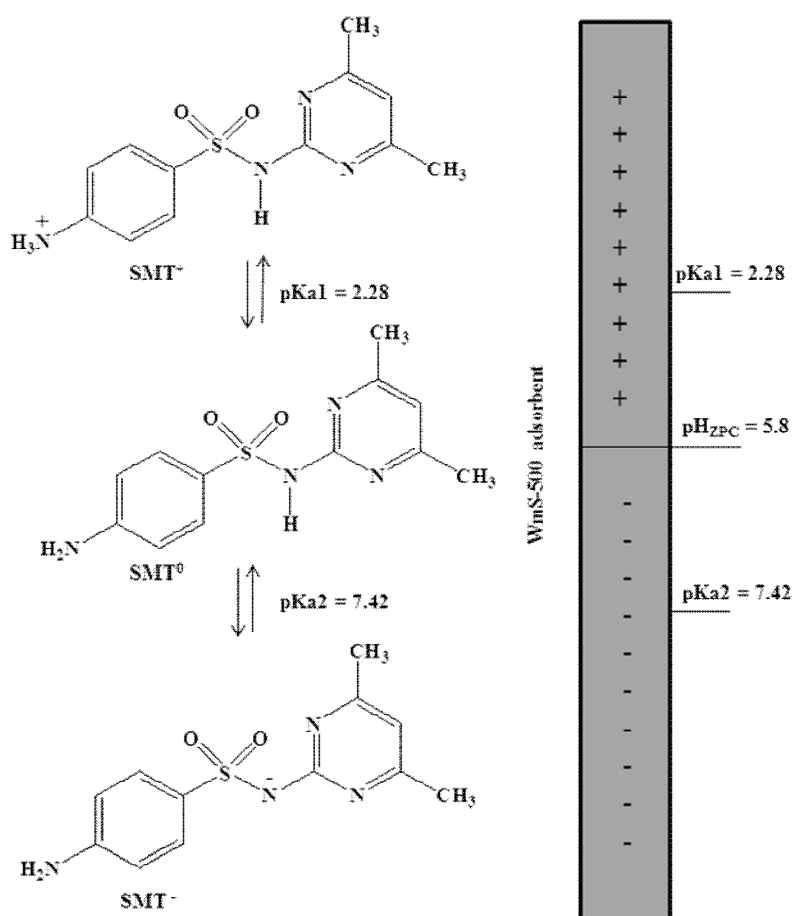


Fig. 6. State speciation and surface charge.



poor compounds [29]. The possibility of interaction with EDA has been considered in further research on the adsorption of SMT [24,28,29]. To better understand the adsorption mechanism of SMT on WmS-500 adsorbent, herein, the effect of solvent on SMT adsorption onto WmS-500 was studied.

The position, intensity and shape of the absorption bands of the compounds in solution depend on the solvent. These changes reflect the WmS-500 and solvent physical interactions that alter the energy difference between the ground state and excited state. The ( $n-\pi^*$ ) transition causes a decrease in wavelength by increasing the polarity of the solvent. The ( $\pi-\pi^*$ ) transition shows that wavelength increases by increasing the polarity of the solvent.

The study of the displacement of the bands by the effect of the polarity of the solvents can help to recognize the nature of the observed transitions. For this reason, the variation of the volume of organic solvents: methanol, acetone, acetonitrile and tetrahydrofuran (THF) while keeping the concentration of antibiotics in the constant solution ( $10 \text{ mg l}^{-1}$ ). The study of the influence of solvents on the adsorbed quantities of this pollutant is represented by the curve in Fig. 7.

It should be noted that the adsorbed quantity decreases as the volume of the solvents increases. This result can be explained by the direct competition of the adsorption sites between the organic solvent and sulfamethazine, which makes it more difficult to adsorb SMT onto the surface of WmS-500. Thus, it is noted that there is a difference between the adsorbed amounts of SMT for each solvent. This can be explained by the polarity that not only affects the separation and affinity of the molecules, but also creates a polar region and reduces the hydrophobicity of the WmS-500 adsorbent surface, leading to a decrease in the adsorption of SMT by WmS-500. The main effects were attributed to the hydrophobic and electrostatic interactions that dominated the adsorption behavior. The hydrophobic interaction decreases with increasing surface solvent levels due to the introduction of the functional group into the surface of WmS-500 adsorbent, which could weaken  $\pi-\pi$  interactions between sulfamethazine and WmS-500. Previous studies have shown that  $\pi-\pi$ , hydrophobic and electrostatic interactions are the predominant mechanisms for adsorption of SMT [28,29].

Figure 8 shows that the sulfamethazine spectrum is capable of interacting with the solvent. This is usually stabilized by the  $\pi-\pi^*$  transition. Stabilization means lower transition energy which leads to the longer wavelength. SMT with atoms likely to interact by  $\pi-\pi^*$  transitions: will see the wavelength of absorption increases if the solvent is more polar. Stabilization is deduced in the polar solvents. It is found that SMT molecule has a chromophore group; substituting the near environment of the chromophore can come to modify the characteristics of this chromophore, the value of maximal wavelength and extinction molar coefficient. Therefore, it appears from Fig. 8 that absorption intensity decreases, so this is the hypochromic effect.

### Adsorption Kinetics

Kinetic models are used to examine the rate of the adsorption process and the potential rate-controlling step. In the present work, the kinetic data obtained from batch studies have been analyzed using pseudo-first-order, pseudo-second-order [30], and Elovich and intra-particle diffusion models [31]. The values of the parameter of pseudo-first-order  $k_1$  and  $q_e$  were evaluated experimentally and calculated using the slope and intercept of plots of  $\log(q_e - q_t)$  vs.  $t$ . The pseudo-second-order adsorption parameters  $q_e$  and  $k_2$  were determined by plotting  $t/q_t$  vs.  $t$ . The intra-particle-diffusion adsorption parameters  $C$  and  $k_1$  were determined by plotting  $t^{1/2}$  vs.  $q_t$ . The Elovich kinetic adsorption parameters  $q_e$  and  $\beta$  were determined by plotting  $\ln(t)$  vs.  $q_t$ .

The results of Table 3 show that the correlation coefficients of the pseudo-second-order kinetic model are very close to 1 compared to the other models. Also, the values of adsorbed quantities  $q_{e,cal}$  calculated by this model are comparable to that experimental  $q_{e,exp}$  which shows that the adsorption kinetics is described by the pseudo-second-order kinetic model. This model assumes that the limiting step, adsorption is chemisorption, which involves electron exchanges at the solid-liquid interface [30]. The kinetic constant value  $k_2$  shows that the retention of SMT by WmS-500 adsorbent is fairly rapid.

The estimated  $q_e$  values of the Elovich kinetic model showed that the sorption could be explained by this model. The Elovich model derived from the kinetics of the chemical reaction suggests that the curves do not pass

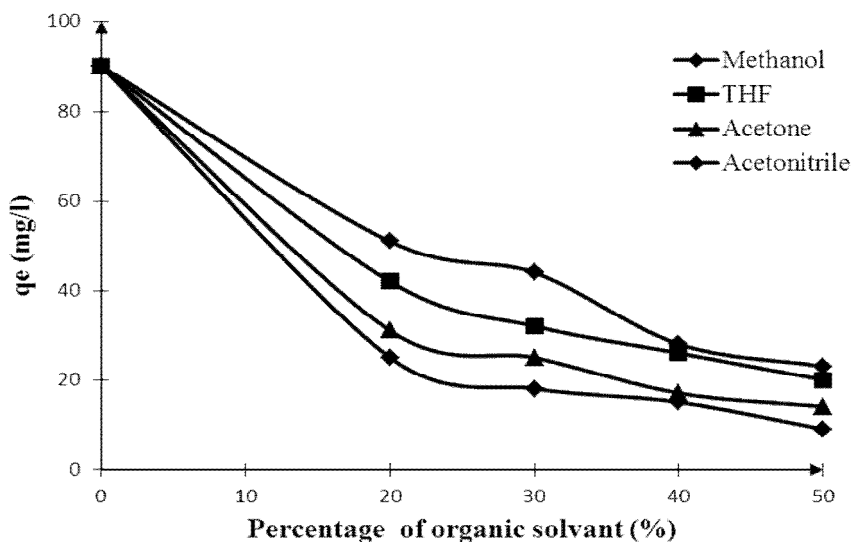


Fig. 7. Effect of organic solvent on the adsorption capacity of SMT by WmS-500 adsorbent.

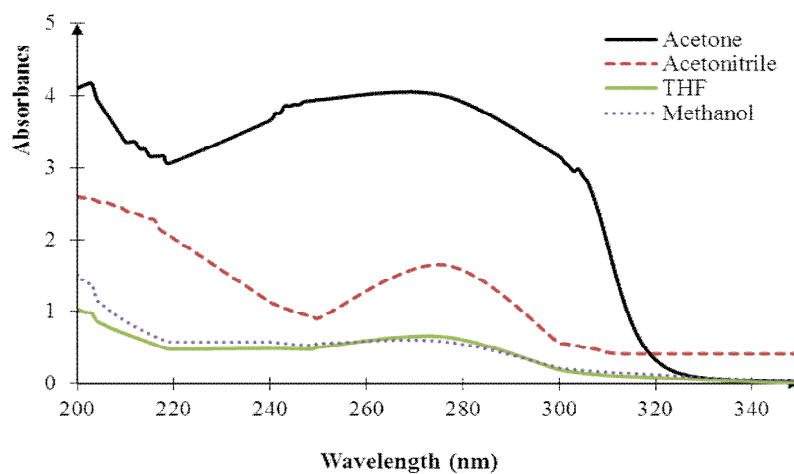


Fig. 8. Sulfamethazine spectrum according to solvents.

through the origin; there is a certain degree of control of the boundary layer between the SMT in solution and WmS-500 adsorbent. This control of the boundary layer is believed to be related to the rate control mechanism and involves  $\pi$ - $\pi$  interactions between the SMT in solution and WmS-500 adsorbent sites, which is in a good agreement with the other results found.

The intra-particle diffusion curve indicates that the diffusion of SMT towards the surface of WmS-500

adsorbent occurs in three phases. The initial steep phase represented the surface diffusion. The second, less steep phase represented the gradual sorption of SMT in which intra-particle diffusion into the pores was limiting, and the third phase where the equilibrium was reached. The curve did not cross the origin; intra-particle diffusion was not the only limiting step. Three processes were controlling the sorption rate of SMT, but only one predominates at any time. The values of the intra-particle diffusion model

**Table 3.** Modeling Kinetics Parameters for SMT Antibiotic onto WmS-500 Adsorbent

Kinetics model	Model parameters	SMT antibiotic
Pseudo first order	$q_e$ ( $\text{mg g}^{-1}$ )	7.890
	$k_1$ ( $\text{min}^{-1}$ )	0.028
	$R^2$	0.875
Pseudo second order	$q_e$ ( $\text{mg g}^{-1}$ )	91.43
	$k_2$ ( $\text{g mg}^{-1} \text{min}^{-1}$ )	0.200
	$R^2$	0.999
Intra-particle diffusion	$C$ ( $\text{mg g}^{-1}$ )	45.15
	$K_i$	5.090
	$R^2$	0.724
Elovich	$q_e$ ( $\text{mg g}^{-1}$ )	79.60
	$\beta$	0.022
	$R^2$	0.878
	$q_{\text{exp}}$ ( $\text{mg g}^{-1}$ )	90.78

**Table 4.** Constants of Various Isotherms Models for the SMT Adsorption onto WmS-500 Adsorbent

Langmuir	$q_e$	115.9
	( $\text{mg g}^{-1}$ )	
	$R_L$	0.3448
	$R^2$	0.993
Freundlich	$1/n$	2.38
	$K_F$	0.876
	$R^2$	0.921
Dubinin-Radushkevich	$q_e$ ( $\text{mg g}^{-1}$ )	80.16
	$K_D$	$5 \times 10^{-7}$
	$R^2$	0.840

constants are shown in Table 3. The C values indicate the thickness of the boundary layer that has been observed to be very small for these soils; and these low C values suggest that surface diffusion plays less of a role as a speed limiting step in the overall sorption process.

### Adsorption Isotherms

The adsorption equilibrium is significant in describing the adsorption effect. The parameters derived from the representation models provide important information on the adsorption mechanisms. The adsorption capacity at different equilibrium aqueous concentrations could be given by the adsorption isotherm. In this research, to analyze the characteristics of adsorption isotherms, three models including Langmuir, Freundlich and Dubinin-Radushkevich (D-R) were used to analyze the equilibrium adsorption data. The linearized Langmuir isotherm model can be described as the following equation [32]:

$$\frac{C_e}{q_e} = \frac{1}{q_m K_L} + \frac{1}{q_m} C_e$$

where  $K_L$  ( $M^{-1}$ ) is the Langmuir adsorption constant related to the adsorption energy,  $q_m$  and  $q_e$  ( $mg\ g^{-1}$ ) are the maximum and equilibrium adsorption capacity ( $mg\ g^{-1}$ ), respectively.  $K_L$  indicates the affinity for the binding of reactive dyes. A high  $K_L$  value indicates a high affinity, while  $q_m$  represents the monolayer saturation at equilibrium when the surface is fully covered with antibiotic molecules and assists in the explanation of adsorption performance. By plotting  $C_e/q_e$  against  $C_e$ , the values of  $q_m$  can be obtained from the slope. Moreover, the obtained values of  $q_m$  and  $R^2$  for the adsorption of antibiotic are presented in Table 4. After obtaining  $q_m$ , the value of  $K_L$  is the ability to be determined from the intercept of the plot.

To confirm the favorability of the adsorption process, the separation factor  $R_L$  was calculated by the following Eq. (4) [32]:

$$R_L = \frac{1}{1 + K_L C_0}$$

where the adsorption process to be either unfavorable ( $R_L > 1$ ), linear ( $R_L = 1$ ), favorable ( $0 < R_L < 1$ ) or

irreversible ( $R_L = 0$ ). Here,  $R_L$  values for the adsorption of antibiotic are less than 1 and greater than zero indicating favorable adsorption.

Freundlich model is applied to adsorption on heterogeneous surfaces with the interaction between the adsorbed molecules [33]. The linearized form of the Freundlich isotherm model is given as the following equation [33]:

$$\log(q_e) = \log(K_f) + \frac{1}{n} \log(C_e) \tag{5}$$

where  $K_F$  ( $M^{-1}$ ) is the Freundlich constant and  $1/n$  is the heterogeneity factor. By plotting  $\ln(q_e)$  vs.  $\ln(C_e)$ , the values of  $n$  and  $K_F$  can be obtained from the slope and the intercept of the linear plot.

The linearized form of the D-R isotherm model can be illustrated as Equations [34]:

$$\ln(q_e) = \ln(q_m) - B\varepsilon^2 \tag{6}$$

$$\varepsilon = RT \cdot \ln\left(1 + \frac{1}{C_e}\right) \tag{7}$$

where  $q_m$  ( $mg\ g^{-1}$ ) is a constant in the D-R isotherm model which is related to adsorption capacity,  $K_D$  ( $mol^2\ kJ^{-2}$ ) is a constant related to the mean free energy of adsorption,  $R$  ( $J\ mol^{-1}\ K^{-1}$ ) is the gas constant, and  $T$  (K) is the absolute temperature. By plotting  $\ln(q_e)$  against  $\varepsilon$ , it is possible to obtain the value of the D-R constants  $K_D$  and  $q_s$ .

Results shown in Table 4 describe the constants of Langmuir, Freundlich and D-R isotherms concerning the adsorption of SMT onto WmS-500. For correlation coefficients, high  $R^2$  are derived by fitting experimental data into the Langmuir isotherm model and the Freundlich isotherm model as compared with the D-R isotherm model. These suggest that both the Langmuir isotherm model and the Freundlich isotherm model can generate a satisfactory fit to the experimental data, while the D-R isotherm model cannot. As shown, the values of maximum adsorption capacity determined using the Langmuir model are near the experimental values for SMT onto WmS-500. They were explained by the Langmuir model indicating the following assumptions: monolayer sorption (each site can hold at most

**Table 5.** Thermodynamic Data for the Adsorption of SMT onto WmS-500 Adsorbent

Temperature	$\Delta G^\circ$ (J mol <sup>-1</sup> )	$\Delta H^\circ$ (J mol <sup>-1</sup> )	$\Delta S^\circ$ (J K <sup>-1</sup> mol <sup>-1</sup> )
298	-538.8		
308	-556.6		
318	-574.4	-8.36	1.78
328	-592.2		

one molecule), the surface containing the adsorbing sites is a perfectly flat plane with no corrugations, indicating that the surface is homogeneous, also all sites are equivalent and the adsorption process is favorable as well, because ( $0 < R_L < 1$ ).

### Thermodynamic Study

Thermodynamic data reflect the feasibility and favorability of the adsorption process. Parameters such as free energy change ( $\Delta G^\circ$ ), enthalpy change ( $\Delta H^\circ$ ) and entropy change ( $\Delta S^\circ$ ) can be determined by the change of equilibrium temperature [22]. The free energy change of the adsorption reaction is given as:

$$\Delta G^\circ = -RT \ln(K_c) \quad (8)$$

where  $\Delta G^\circ$  is the free energy change (kJ mol<sup>-1</sup>), R is the universal gas constant (8.314 J mol<sup>-1</sup> K<sup>-1</sup>), T is the absolute temperature (K), and  $K_c$  states the equilibrium constants ( $q_e/C_e$ ). The values of  $\Delta H^\circ$  and  $\Delta S^\circ$  can be calculated from the following equation:

$$\ln(K_c) = -\frac{\Delta H^\circ}{RT} + \frac{\Delta S^\circ}{R} \quad (9)$$

where  $K_c$  is plotted against  $1/T$ , a straight line with the slope ( $-\Delta H^\circ/R$ ) and intercept ( $\Delta S^\circ/R$ ) are given.

The calculated thermodynamic parameters for antibiotic are presented in Table 5. For sulfamethazine, the negative values of  $\Delta G^\circ$ , at all temperatures, confirmed the thermodynamic feasibility. The negative value of  $\Delta H^\circ$

shows that the adsorption is exothermic in nature. The positive value of  $\Delta S^\circ$  suggests that the degree of randomness state at the solid/solution interface increased during the adsorption of SMT onto WmS-500 adsorbent. On the other side, the negative values of  $\Delta G^\circ$  and its decrease with temperature indicate an increase of the disorder during adsorption, the random appearance increases at the solid-solution interface during this fixation process, this can be explained by the redistribution of energy between the adsorbent and the adsorbate [34-36].

### CONCLUSIONS

The results of this study show that WmS-500 can be successfully used as a low cost and eco-friendly adsorbent for the removal of SMT from aqueous solution. The WmS-500 interactions were very fast in the first 5 min and attained equilibrium within 60 min for SMT. The kinetics was very close to the pseudo-second-order model, and the Langmuir isotherm was the best model to describe the phenomenon in the single and binary systems. Pointed to the non-specific and energetically non-uniform nature of the adsorption sites. Then, we studied the solvent effects to show that the electron-donor-acceptor interaction is the main adsorption mechanism for antibiotics and that the adsorption capacity increases with the increase in dipolar moment of the solvent.

### REFERENCES

- [1] Jiangdong, D.; Atian, X.; Ruilong, Z.; Wenna, G.;

- Zhongshuai, C.; Sujun, T.; Chunxiang, L.; Yongsheng, Y., Scalable preparation of hierarchical porous carbon from lignin for highly efficient adsorptive removal of sulfamethazine antibiotic. *J. Mol. Liq.* **2017**, *256*, 203-212, DOI: 10.1016/j.molliq.2018.02.042.
- [2] Zhang, L.; Wang, Y.; Jin, S.; Lu, Q.; Ji, J., Adsorption isotherm, kinetic and mechanism of expanded graphite for sulfadiazine antibiotics removal from aqueous solutions. *Environ. Technol.* **2017**, *38*, 2629-2638, DOI: 10.1080/09593330.2016.1272637.
- [3] Yi, L.; Lin, X.; Michal, R.; Yuqiu, W.; Hao, Z.; Pedro, J. J. A., Occurrence and transport of tetracycline, sulfonamide, quinolone, and macrolide antibiotics in the Haihe River Basin, China. *Environ. Sci. Technol.* **2011**, *45*, 1827-1833, DOI: 10.1021/es104009s.
- [4] Zhou, L.; Ying, G.; Liu, S.; Zhang, R.; Lai, H.; Chen, Z.; Pan, C., Excretion masses and environmental occurrence of antibiotics in typical swine and dairy cattle farms in China. *Sci. Total. Environ.* **2013**, *444*, 183-195, DOI: 10.1016/j.scitotenv.2012.11.087.
- [5] Thai-Hoang, L.; Charmaine, N.; Ngoc, H. T.; Hongjie, C.; Karina, Y. H. G., Removal of antibiotic residues, antibiotic resistant bacteria and antibiotic resistance genes in municipal wastewater by membrane bioreactor systems. *Water. Res.* **2018**, *145*, 498-508, DOI: 10.1016/j.watres.2018.08.060.
- [6] Harrabi, M.; Giustina, S. V. D.; Aloulou, F.; Mozaz, S. R.; Barceló, D.; Elleuch, B., Analysis of multiclass antibiotic residues in urban wastewater in Tunisia. *Nanotechnol. Monit. Manag.* **2018**, *10*, 163-170, DOI: 10.1016/j.enmm.2018.05.006.14.
- [7] Yeong-Joo, C.; Lee-Hyung, K.; Kyung-Duk, Z., Removal characteristics and mechanism of antibiotics using constructed wetlands. *Ecol. Eng.* **2016**, *91*, 85-92, DOI: 10.1016/j.ecoleng.2016.01.058.
- [8] Dai, J.; Pan, J.; Xu, L.; Li, X.; Zhou, Z.; Zhang, R.; Yan, Y., Preparation of molecularly imprinted nanoparticles with superparamagnetic susceptibility through atom transfer radical emulsion polymerization for the selective recognition of tetracycline from aqueous medium. *J. Hazard. Mater.* **2012**, *205*, 179-188, DOI: 10.1016/j.jhazmat.2011.12.056.
- [9] Chen, B.; Liang, X.; Nie, X.; Huang, X.; Zou, S.; Li, X., The role of class I integrons in the dissemination of sulfonamide resistance genes in the Pearl River and Pearl River Estuary, South China. *J. Hazard. Mater.* **2015**, *282*, 61-67, DOI: 10.1016/j.jhazmat.2014.06.010.
- [10] Lillenberg, M.; Yurchenko, S.; Kipper, K.; Herodes, K.; Pihl, V.; Sepp, K.; Lõhmus, R.; Nei, L., Simultaneous determination of fluoroquinolones, sulfonamides and tetracyclines in sewage sludge by pressurized liquid extraction and liquid chromatography electrospray ionization-mass spectrometry. *J. Chromatogr. A* **2009**, *1216*, 5949-5954, DOI: 10.1016/j.chroma.2009.06.029.
- [11] Ling, Q.; Zhiping, Z.; Jiangdong, D.; Ping, M.; Haibin, Z.; Jinsong, H.; Atian, X.; Chunxiang, L.; Yongshen, Yan., Novel N-doped hierarchically porous carbons derived from sustainable shrimp shell for highperformance removal of sulfamethazine and chloramphenicol. *J. Taiwan. Inst. Chem. E* **2016**, *62*, 228-238, DOI: 10.1016/j.jtice.2016.02.009.
- [12] Pow-Seng, Y.; Yan-Ling, C.; Madhavi, S.; Teik-Thye, L., Bimodal N-doped P25-TiO<sub>2</sub>/AC composite: preparation, characterization, physical stability, and synergistic adsorptive-solar photocatalytic removal of sulfamethazine. *Appl. Catal. A-Gen.* **2012**, *427*, 125-136, DOI: 10.1016/j.apcata.2012.03.042.
- [13] Quanquan, Y.; Guangcai, C.; Jianfeng, Z.; Helian, L., Adsorption of sulfamethazine by multi-walled carbon nanotubes: effects of aqueous solution chemistry. *RSC ADV.* **2015**, *5*, 25541-25549, DOI: 10.1039/C4RA15056B.
- [14] Danlian, H.; Xi, W.; Chen, Z.; Guangming, Z.; Zhiwei, P.; Jin, Z.; Min, C.; Rongzhong, W.; Zhengxun, H.; Xiang, Q., Sorptive removal of ionizable antibiotic sulfamethazine from aqueous solution by graphene oxide-coated biochar nanocomposites: Influencing factors and mechanism. *Chemosphere* **2017**, *186*, 414-421, DOI: 10.1016/2017.07.154.
- [15] Jiu-Qiang, X.; Sanjay, G.; Mayur, B. K.; Ki-Jung, P.; Hyun-Seog, R.; Moonis, A. K.; Byong-Hun, J., Toxicity of sulfamethazine and sulfamethoxazole and their removal by a green microalga, *Scenedesmus*

- obliquus. *Chemosphere* **2019**, *218*, 551-558, DOI: 10.1016/j.chemosphere.2018.11.146.
- [16] Senar, A.; Mehmet, E. A.; Fatma, B.; Arzu, U., Removal of antibiotics from aqueous solution by using magnetic Fe<sub>3</sub>O<sub>4</sub>/red mud-nanoparticles. *Sci. Total. Environ.* **2019**, *670*, 539-546, DOI: 10.1016/j.scitotenv.2019.03.205.
- [17] Anushka, U. R.; Meththika, V.; Mahtab, A.; Dong-Cheol, S.; Ju-Sik, C.; Sung-Eun, L.; Sang, S. L.; Yong, S. O., Enhanced sulfamethazine removal by steam-activated invasive plant derived biochar. *J. Hazard. Mater.* **2015**, *290*, 43-50, DOI: 10.1016/j.jhazmat.2015.02.046.15.
- [18] Ying, L.; Xiaohui, L.; Guodong, Z.; Tao, M.; Tingqin, D.; Yong, Y.; Shaoyong, L.; Weiliang, W., Adsorptive removal of sulfamethazine and sulfamethoxazole from aqueous solution by hexadecyl trimethyl ammonium bromide modified activated carbon. *Colloid. Surface. A* **2019**, *564*, 131-141, DOI: 10.1016/j.colsurfa.2018.12.041.
- [19] Ijaz, H.; Yang, L.; Junwen, Q.; Jiansheng, L.; Xiuyun, S.; Jinyou, S.; Weiqing, H.; Lianjun, W., Synthesis of magnetic yolk-shell mesoporous carbon architecture for the effective adsorption of sulfamethazine drug. *Microporous. Mesoporous. Mater.* **2018**, *255*, 110-118, DOI: 10.1016/j.micromeso.2017.07.027.
- [20] Muhammad, M.; Isa, M. T.; Lukman, I.; Muhammad, N.; Muhammad, S.; Rizwan, A.; Rehan, H., Influence of PZC (point of zero charge) on the static adsorption of anionic surfactants on a Malaysian sandstone. *J. Disper. Sci. Technol.* **2014**, *35*, 343-349, DOI: 10.1080/01932691.2013.785362.
- [21] Sha, L.; Xueyi, G.; Qinghua, T., Adsorption of Pb<sup>2+</sup> and Zn<sup>2+</sup> from aqueous solutions by sulfured orange peel. *Desalination* **2011**, *275*, 212-216, DOI: 10.1016/j.desal.2011.03.001.
- [22] Yang-Chuang, C.; Dong-Hwang, C.; Adsorption Kinetics and Thermodynamics of Acid Dyes on a Carboxymethylated chitosan-conjugated magnetic nano-adsorbent. *Water. Environ. Res.* **2005**, *5*, 254-261, DOI: 10.1002/mabi.200400153.
- [23] Panpan, L.; Xin, Z.; Baolin, P.; Mingjian, W.; Zhuoyong, Z.; Peter, B. H., Classification of sand grains by terahertz time-domain spectroscopy and chemometrics. *Int. J. Environ. Sci.* **2019**, *13*, 143-160, DOI: 10.1007/s41742-018-0159-y.
- [24] El Kassimi, A.; Regti, A.; Laamari, R.; El Haddad, M., Adsorptive removal of anionic dye from aqueous solutions using powdered and calcined vegetable wastes as low-cost adsorbent. *J. Basic Appl. Sci.* **2018**, *25*, 93-102, DOI: 10.1080/25765299.2018.1517861.
- [25] Park, J. Y.; Huwe, B., Effect of pH and soil structure on transport of sulfonamide antibiotics in agricultural soils. *Int. J. Environ. Pollut.* **2016**, *213*, 561-570, DOI: 10.1016/j.envpol.2016.01.089.
- [26] Kang, S. I.; Bae, Y. H., Ph-induced solubility transition of sulfonamide-based polymers. *J. CR* **2002**, *80*, 145-155, DOI: 10.1016/S0168-3659(02)00021-4.
- [27] Jina, Z.; Zhang, Q.; Chena, J.; Huang, S.; Hua, L.; Zenga, Y. J.; Zhang, H.; Ruana, S.; Ohno, T., Hydrogen bonds in heterojunction photocatalysts for efficient charge transfer. *Appl. Catal. B-Environ.* **2018**, *234*, 198-205, DOI: 10.1016/j.apcatb.2018.04.057.16
- [28] Ma, X.; Agarwal, S., Adsorption of emerging ionizable contaminants on carbon nanotubes: advancements and challenges. *J. Mol. Liq.* **2016**, *21*, 712-719, DOI: 10.3390/molecules21050628.
- [29] Dai, J.; Xie, A.; Zhang, R.; Ge, W.; Chang, Z.; Tian, S.; Li, C.; Yan, Y., Scalable preparation of hierarchical porous carbon from lignin for highly efficient adsorptive removal of sulfamethazine antibiotic. *J. Mol. Liq.* **2018**, *256*, 203-212, DOI: 10.1016/j.molliq.2018.02.042.
- [30] Arris, S.; Lehocine, M. B.; Meniai, A. H., Sorption study of chromium sorption from waste water using cereal by-products. *Int. J. Hydrog. Energy* **2014**, *41*, 10299-10310, DOI: 10.1016/j.ijhydene.2014.09.147.
- [31] Ghazy, M.; Harby, K.; Askalany, A. A.; Saha, B. B., Adsorption isotherms and kinetics of activated carbon/difluoroethane adsorption pair: theory and experiments. *Inr. J. Refrig.* **2016**, *70*, 196-205, DOI: 10.1002/apj.2372
- [32] Saha, B. B.; El-Sharkawy, I. I.; Thorpe, R.; Critoph, R. E., Accurate adsorption isotherms of R134a onto activated carbons for cooling and freezing applications. *Inr. J. Refrig.* **2012**, *35*, 499-505, DOI: 10.1016/j.ijrefrig.2011.05.002.

- [33] Wanga, C.; Boithias, L.; Ningd, Z.; Hana, Y.; Sauvagee, S.; Péreze, J. M. S.; kuramochid, K.; Hatano, R., Comparison of langmuir and freundlich adsorption equations within the swat-k model for assessing potassium environmental losses atbasin scale. *Agric. Water. Manag.* **2016**, *180*, 205-211, DOI: 10.1016/j.agwat.2016.08.001.
- [34] Lodewyckx, P.; Verhoeven, L., The applicability of the dubinin-radushkevich equation to the very low pressure region of isotherms of various microporous solids. *Stud. Surf. Sci. Catal.* **2002**, *144*, 731-735, DOI: 10.1016/S0167-2991(02)80203-8.
- [35] Shukla, P. R.; Chong, S.; Pan, G. T.; Wang, S.; Ang, M.; Rudolph, V., Adsorption of phenolic contaminants from water on activated carbon: An insight into single and multicomponent adsorption isotherms. *Asia. Pac. J. Chem. Eng.* **2019**, *14*, DOI: 10.1002/apj.2372.
- [36] He, J.; Ma, Y.; He, J.; Zhao, J.; Yu, J. C., Photooxidation of azo dye in aqueous dispersions of H<sub>2</sub>O<sub>2</sub>/α-FeOOH. *Appl. Catal. B* **2002**, *39*, 211-220, DOI: 10.1016/S0926-3373(02)00085-1.